HHS Public Access

Author manuscript

J Immunol. Author manuscript; available in PMC 2022 January 01.

Published in final edited form as:

J Immunol. 2021 July 01; 207(1): 5–14. doi:10.4049/jimmunol.2100061.

MHC Class II presentation is affected by polymorphism in the *H2-Ob* gene and additional loci

Emily Cullum[*], **Austin M. Graves**[†], **Vera L. Tarakanova**[‡], **Lisa K. Denzin**[‡,¶], **Tatyana Golovkina**[*,‖,#]

[*]Committee on Immunology, University of Chicago, Chicago, IL, 60637

[†]Graduate School of Biomedical Sciences, Rutgers, The State University of NJ, New Brunswick, NJ, 08901

[‡]Microbiology and Immunology, Cancer Center, Medical College of Wisconsin, Milwaukee, WI 53226

[¶]Child Health Institute of NJ, Department of Pediatrics, Rutgers Robert Wood Johnson Medical School, The State University of NJ, New Brunswick, NJ, 08901

[‖]Committee on Microbiology, University of Chicago, Chicago, IL, 60637

[#]Department of Microbiology, University of Chicago, Chicago, IL, 60637

Abstract

Pathogen-derived peptides are loaded on Major Histocompatibility Class II (MHCII) and presented to $CD4^+$ T cells for their activation. Peptide loading of MHCII occurs in specialized endosomal compartments and is controlled by the non-classical MHCII molecules H2-M and H2-O, which are both constitutive αβ heterodimers. H2-M catalyzes MHCII peptide loading, whereas H2-O modulates H2-M activity by acting as an MHCII mimic. Recently, we discovered that the *H2-Ob* allele inherited by retrovirus-resistant I/LnJ mice results in nonfunctional H2-O. I/LnJ H2-O binds to but does not inhibit H2-M. Compared to H2-Oβ from virus-susceptible mice, H2-Oβ from I/LnJ mice has 4 unique amino acid (AA) substitutions: three in the immunoglobulin (Ig) domain and one in the cytoplasmic tail. Here we show that the three AAs in the Ig domain of I/LnJ Oβ are critical for the H2-O inhibitory activity of H2-M. Unexpectedly, we found that MHCII presentation was significantly different in antigen presenting cells from two closely related mouse strains, B6J and B6N, which carry identical alleles of MHCII, H2-O, and H2-M. Using a positional cloning approach, we have identified two loci, polymorphic between B6J and B6N, that mediate the difference in MHCII presentation. Collectively these studies reveal extra complexity

Address correspondence to Dr. T. Golovkina, Tel. (773) 8347988; tgolovki@bsd.uchicago.edu.

Author contributions

E.C. assisted in generation and phenotyping of various B6.*Ob* KI mice, genetic analysis of B6J, B6N and CAST mice, flow cytometry experiments, and biochemical experiments, and contributed to the discussion of results and writing and editing the manuscript. L.K.D. designed and performed BMC experiments, flow cytometry experiments, and biochemical experiments and also contributed to the discussion of experimental design and results and writing of the manuscript. A.G. performed flow cytometry experiments. V.L.T. contributed to the discussion of experimental design and editing the manuscript. T.G. conceived the project, guided the genetic crosses, contributed to all experiments and wrote the manuscript.

Disclosures

The authors have no financial conflicts of interest.

in MHCII/H2-M/H-2O interactions that likely involve yet to be identified modulators of the pathway.

Introduction

The individual outcomes that follow exposure to viral pathogens vary significantly among individuals in both humans and animals. In part, such variations are determined by genetic diversity of the immune response. Similar to mice from other strains, I/LnJ mice become infected with retroviruses from distinct genera, such as Mouse Mammary Tumor Virus (MMTV) and Murine Leukemia Virus (MuLV), but unlike mice from other strains I/LnJ mice produce virus-neutralizing antibodies (Abs) and shed uninfectious virions (1, 2). We found that this unique mechanism of retroviral resistance was controlled by a single recessive locus, virus infectivity controller 1 (*vic1*), mapped to the MHC locus on Chromosome 17 (3), which functioned in bone marrow (BM)-derived cells to drive the Ab response (4).

The gene encoding Vic1 was subsequently identified as *Ob* based on polymorphism found in this gene in virus-susceptible and virus-resistant mice (5). *Ob* encodes the β chain of the highly conserved MHCII-like αβ obligate heterodimer H2-O (6), which is a negative regulator of MHCII-peptide presentation (7). Peptide loading of MHCII molecules is catalyzed in specialized endosomes by H2-M, another MHCII-like αβ heterodimer. H2-M binds to MHCII and replaces MHCII-associated invariant chain peptides (CLIP) with high affinity, pathogen-derived peptides generated by lysosomal proteases, such as cathepsin L and S. H2-O binds to H2-M and acts as an MHCII mimic, blocking the ability of H2-M to bind to MHCII and catalyze MHCII peptide loading. This concept is based on the crystal structure of the DM/DO (human homologues of H2-M and H2-O) complex (8) and a plethora of other supporting biochemical data from numerous groups (9–15).

Based on the recessive nature of the Ab responses in I/LnJ mice, the I/LnJ *Ob* allele was presumed to be a loss-of-function allele. In support of this, mice from other genetic backgrounds with targeted *Ob* deletion were capable of producing retrovirus-neutralizing Abs similar to I/LnJ mice and antigen presenting cells (APCs) expressing I/LnJ Oβ exhibited increased antigen presentation (5). In the absence of H2-O, H2-M is uninhibited and results in small changes in the MHCII-bound peptidome favoring presentation of high affinity peptides (14, 16). Thus, these small changes appear to be sufficient to direct potent virus-neutralizing Ab responses (5) most likely due to enhanced presentation of high affinity viral peptides.

Although the I/LnJ *Ob* was shown to be null, biochemical analyses revealed that I/LnJ mice had Oβ protein levels that were similar to Oβ levels in susceptible mice and produced H2-O that associated with H2-M (5). Thus, the I/LnJ *Ob* allele resulted in H2-O that was capable of binding to H2-M but yet did not modulate H2-M-mediated peptide loading.

We have also identified human *DOA* and *DOB* alleles with altered DO function, a few of which phenocopied I/LnJ H2-O as they inefficiently inhibited DM, despite binding to DM (5, 17). Therefore, these unexpected results challenged the current paradigm that

H2-O functions alone to inhibit H2-M activity and suggested existence of unknown factors contributing to H2-O function. Using a genetic approach, we have identified three AA mutations within the Ig of *Ob* which control H2-O function. We have also discovered two new non-MHC-linked loci which modify MHCII antigen presentation.

Materials and Methods

Mice

I/LnJ, C57BL/6J (B6J), C57BL/6NJ (B6N), and CAST/Ei were purchased from The Jackson Laboratory (TJL) and bred at The University of Chicago. B6J.*H2-Ob*$^{-/-}$ mice (line 134) and B6$^{vic1I/LnJ}$ congenic mice carrying the non-recombinant virus infectivity controller 1 (*vic1*) locus from I/LnJ mice were generated by us and have been described previously (5). C3H/HeN MMTV-free mice were originally purchased from the National Cancer Institute Frederick Cancer Research Facility, Frederick, MD, and maintained at The University of Chicago. In addition, colonies of B6J, B6J.*H2-Oa*$^{-/-}$ (15), B6J.*H2-Ob*$^{-/-}$ (5), B6J.*H2-Ma*$^{-/-}$ (18) were maintained at the animal facility of Rutgers University. For bone marrow chimera (BMC) experiments, B6N, B6J and B6.129S2-Ighm^{tm1Cgn}/J (B6J.μMT) were purchased from TJL and maintained in the Rutgers University Animal Facility.

All mice were raised in a specific pathogen-free environment. Mice of both sexes were used at 1:1 ratio in all experiments. The studies described here have been reviewed and approved by the Animal Care and Use Committees at The University of Chicago and Rutgers University which are both accredited by the Association for Assessment and Accreditation of Laboratory Animal Care (AAALAC).

Production of B6 Ob knockin mice

B6J mice with single and combination amino acid (AA) substitutions found in I/LnJ Oβ were generated using a CRISPR/Cas9 approach. Two guides (sgRNA: CTGTAGATGTCACCAAGCTC and sgRNA: CACTTGACACTTATGTCCCC) were used to target the immunoglobulin domain to replace S, V, L with N, I, H AAs and two guides (sgRNA: AGAATGAGACTCTCTCTTG and sgRNA: GATCTTACTAGGGTTGAGAA) were used to target the cytoplasmic domain to replace ES with KL. Guide sites were identified using Integrated DNA Technologies' selection tool (https://www.idtdna.com/site/order/designtool/index/CRISPR_CUSTOM). Individual guide sites were selected based on their on-target scores and off-target scores. The 500bp ssDNA oligos containing sequences corresponding to the knockin (KI) AAs were co-injected with the RNA guides and Cas9 into fertilized B6J embryos at Transgenic/ES Cell Technology Mouse Core Facility at The University of Chicago and at TJL. The founder mice were identified by PCR. The carriers of the KI *Ob* alleles were bred to B6J mice for two generations and heterozygous mice from each line were intercrossed to produce *Ob* KI homozygous mice. Genomic DNA and splenic cDNA produced from the *Ob* KI alleles were sequenced to confirm mutations. Wild type (WT/WT and WT/KI) control B6J mice were generated from either breeding the colony of B6J mice or from breeding *Ob*.KI/WT × *Ob*.KI/WT mice.

Viral strains and infection

MMTV(LA), a naturally occurring exogenous virus (19), was propagated in C3H/HeN mice. Virus was isolated from the skim milk of lactating females via a series of centrifugation including a 30% sucrose cushion centrifugation. Virions were resuspended in PBS and injected intraperitoneally (i. p.). Each mouse received an equivalent of 20 ul of milk. MMTV(LA) consists of three different exogenous MMTVs, BALB2, BALBLA, and BALB14, with Vβ2-, Vβ6-, and Vβ14-specific superantigens (SAgs), respectively (19, 20). The Vβ6-specific SAg encoded by BALBLA can be presented by both the I-E and I-A molecules of MHC-II and thus, is capable of efficiently infecting I-E-negative mice, like B6 mice (21). All MMTV-infected mice demonstrate deletion of SAg-cognate T cells after 8 weeks post infection (5, 22) and thus, deletion of $CD4^+V\beta6^+$ SAg-cognate T cells was used to confirm MMTV infection. Fluorescence-activated cell sorter (FACS) analysis of peripheral blood lymphocytes was used to measure T cell deletion rates. MMTV(LA)-injected mice were considered to be infected if the percentages of their $CD4^+V\beta6^+$ T cells among peripheral $CD4^+$ T cells were decreased by more than 50% compared to the percentages in uninfected mice.

ELISA

To detect MMTV-specific Abs in mouse sera, an enzyme-linked immunosorbent assay (ELISA) was performed as previously described (1, 2, 23). All sera were used at 1×10^{-2} dilution. A mixture of mouse IgGs-specific and IgG2c-specific secondary antibodies coupled to horseradish peroxidase (Jackson ImmunoResearch) were used to detect anti-virus Abs. Backgrounds obtained from incubation with secondary Abs alone were subtracted from the values obtained from sera of infected mice.

Purification of B cells

B cells were purified from the spleens of the indicated strains of mice using biotin-conjugated Ab specific for CD19 (eBiosciences) followed by MACS (Miltenyi Biotec) using streptavidin-conjugated or α-biotin microbeads according to the manufacturer's protocol. Purified B cells were >95% pure as determined by FACS analysis.

FACS analysis

The following monoclonal Abs for FACs analysis were purchased from eBiosciences or BD Biosciences: CD19-PE (clone 1D3), CD11c-PE-Cy7 (clone HL3), MHCII-biotin (clone M5/114) and CD3-PerCP-Cy5.5 (clone 145–2C11). Strepavidin-Alexa 647 was purchased from Molecular Probes. The α-Oβ cytoplasmic tail specific mAb Mags.Ob3 (24), the α-H2-M specific mAb 2C3A (24) and the $I\text{-}A^b$-CLIP-specific monoclonal Ab 15G4 (15) (provided by A. Rudensky, Memorial Sloan Kettering Cancer Center) were purified from bioreactor supernatants using standard Protein G chromatography and then conjugated with Alexa 647, Alexa 488, or biotin, respectively (ThermoFisher Scientific).

Single cell suspensions of splenic cells were blocked with mouse Fc Block (BD Biosciences) plus normal mouse sera and incubated at 4°C with Abs specific for surface proteins for 30 min followed by washing. After washing, cells were incubated with streptavidin-Alexa 647 for 20 min at room temperature, washed and analyzed by flow

cytometry. For intracellular measurement of H2-M and H2-O, cells were surface stained and fixed and permeabilized (BD Cytofix/Cytoperm™ Fixation/Permeabilization Kit) prior to the addition of Abs, washing, and analysis. For FACS analysis where both splenic B cells and dendritic cells were analyzed, spleens were digested in 400 U/ml collagenase D and 100 mg/ml DNase I for 30 min at 37°C prior to blocking and staining. Data was acquired using a BD LSRII cytometer and analyzed using FlowJo software (BD Biosciences). Dead cells (DAPI or Zombie dye; BioLegend) and doublets were excluded from analyses. For experiments analyzing only splenic B cells, B cells were identified as $CD19^+$. For experiments analyzing both B cells and DCs, B cells were identified as $CD3^-$ $CD11c^-$ and $CD19^+$ and DCs identified as $CD3^-$ $CD19^-$ and $CD11c^+$. Staining to measure MHCII and MHCII-CLIP (I-A^b-CLIP) were always performed as two separate stains since the individual Abs to each of these species interfered when stained simultaneously. To correct for small differences in total MHCII levels among different samples, the ratio of MHCII-CLIP:(total) MHCII was calculated by dividing the gMFI obtained for MHCII-CLIP by that obtained for MHCII for each independent sample. In order to compare multiple independent experiments, the MHCII-CLIP:MHCII ratio for control mice was set to 100%, and the MHCII-CLIP:MHCII ratios for all other samples were normalized to this control. Three-five control mice were included in each independent experiment.

Bone Marrow chimeras

Lineage negative bone marrow (BM) cells from 8–12week old B6J, B6N or B6J.μMT mice were purified using Lineage Cell Depletion Kit (Miltenyi Biotec). The resulting B6J, B6N or a 50:50 mix of B6N + B6J.muMT lineage negative cells were transplanted by intravenous injection (4–7 × 10^5 cells/recipient) into lethally irradiated B6J or B6N recipient mice as indicated. Each mouse received 1200 rads administered as a split dose of 600 rads each with 4 hours between doses. Post-transplant, bone marrow chimeric (BMC) recipient mice were maintained on antibiotic supplemented water for the first two weeks. MHCII-CLIP and MHCII levels were measured on the surface of splenic or peripheral blood B cells from the BMC mice 9–12 weeks post-transplant.

Biochemical Analyses

Purified B cells (5×10^6) from the indicated strains of mice were lysed in 20 mM Tris-HCl, 130 mM NaCl pH 7.4 containing 1.2% CHAPS (ThermoFisher Scientific) and protease inhibitors (Roche Life Science) for 30 min on ice. Following the removal of nuclei and cellular debris by centrifugation, the lysates were transferred to new, pre-chilled tubes and precleared for 30–60 min at 4°C by incubation with 5μg rat or hamster IgG (α-H2-M or α-H2-O immunoprecipitations, respectively) and 25μl of Protein G-Sepharose (GE Healthcare Life Sciences). After centrifugation, 5μg of mAbs specific for the H2-M heterodimer [mAb 2C3A; (24)] or the Oβ cytoplasmic tail [Mags.Ob1; (24)] and 25μl of Protein G Sepharose were added to the precleared lysates. The immunoprecipitations were rotated for 2 hours 4°C and washed three times with 20 mM Tris-HCl, 130 mM NaCl pH 7.4 containing 0.6% CHAPS. The resulting Protein G pellets were stored at −20°C until analysis. Immunoprecipitations from B cells purified from *Ma*- and *Ob*-deficient mice were used as negative controls for the H2-O and H2-M immunoprecipitation.

The precipitated H2-O and H2-M was released from the immunoprecipitation pellets by the addition of Laemmli sample buffer and incubated at 95°C for 5 min prior to separation by 10%–20% gradient SDS-PAGE gels (Criterion, Bio-Rad) and transferred to polyvinylidene fluoride membrane (Millipore). Aliquots of the B cell lysates generated for the immunoprecipitations were also blotted as lysate blotting controls. The lysates were mixed with Laemmli sample buffer containing 20 mM DTT and incubated at 95°C for 5 min prior to analysis by SDS-PAGE.

Membranes were blocked with 1% BSA or 5% skim milk powder and incubated with a rabbit serum to the cytoplasmic tails of Mβ (R.Mb/c; see below) or Oβ [R.Ob/c (24)], the luminal domain of Oβ [R.Obeta1; (5)], a mAb specific for Mα [YoDMA.1; (Fallas et al., 2004)], or β-actin (clone AC-74; Sigma). The blots were washed and bound Abs were detected by incubation with HRP-conjugated goat α-rabbit, -mouse, or -hamster Abs (Jackson ImmunoResearch). After extensive washing blots were developed with SuperSignal West Pico chemiluminescent peroxidase substrate (Pierce Biotechnology) and exposure to film.

To determine the relative levels of Oβ, Mα and Mβ in B cells from the different strains of mice, films were scanned and bands were quantitated using ImageJ (NIH) or Image Studio Lite (LI-COR) software. For the lysate blots, the band density was normalized to that obtained for β-actin to control for differences in loading. To allow data to be combined across multiple independent experiments, the resulting β−actin corrected values were subsequently normalized to the values obtained for H2-O and H2-M from B cells from mice of the indicated control strains. To determine the relative ratio of H2-M and H2-O after immunoprecipitation of H2-O or H2-M, the band density for H2-M was divided by that obtained for H2-O which was then normalized to the value obtained for B cells from mice of the indicated control groups to allow data from independent experiments to be combined.

Polyclonal Abs to the Mβ cytoplasmic tail, were produced in rabbits after multiple immunizations with the Mβ cytoplasmic tail (Mβ/c)-specific peptide (YTPLSGSTYPEGRH) conjugated to keyhole limpet hemocyanin. Mβ/c-specific Abs were purified from the serum by affinity chromatography using Mβ/c peptide-agarose beads.

Virus neutralization

Sera from MMTV-infected mice were tested for their ability to neutralize virus. Each serum diluted at 10^{-1} with PBS was incubated with purified MMTV(LA) for 2 h at room temperature and injected into 2 footpads of BALB/cJ mice. Four days after injection, cells isolated from the draining popliteal lymph node were analyzed by FACS for the percentage of $CD4^+V\beta6^+$ T cells among $CD4^+$ T cells. MMTV-encoded superantigen (SAg) stimulates cognate T cells to proliferate during initial stages of infection (25) which are subsequently deleted. The proliferation of SAg cognate T cells was used as indicator of virus infectivity (26). The amount of MMTV(LA) used was titrated to give an increase from 10% to 25% of SAg-reactive T cells four days after virus injection. Neutralization (%) was calculated as follows: (a-b):(a-c)X100 where a= mean of $CD4^+V\beta6^+$ (%) in mice injected with virus plus sera from uninfected mice, b= mean of $CD4^+V\beta6^+$ (%) in experimental mice and c = mean of $CD4^+V\beta6^+$(%) in uninfected mice.

Quantification and Statistical Analysis

Significance was determined by performing student's unpaired *t*-tests using GraphPad Prism software.

Results

Generation and characterization of B6J.Oβ knockin mice.

Specific amino acid (AA) polymorphisms found in I/LnJ Oβ do not perturb H2-O protein levels or alter the ability of I/LnJ H2-O to associate with H2-M (5). However, despite these seemingly normal biochemical features, I/LnJ H2-O fails to inhibit H2-M function (5). Compared to Oβ from virus-susceptible mice, Oβ from virus-resistant I/LnJ mice has 4 unique missense mutations: three in the Ig domain (S128N, V148I and L167H) and one in the cytoplasmic tail (Ct) (E239K) [(5) and Figure 1A]. We reasoned that determining the polymorphic AA(s) that hinder H2-O function should lead to the elucidation of the mechanism behind the protein's loss-of-function. Thus, using a CRISPR/Cas9 approach we generated Mouse Mammary Tumor Virus (MMTV) susceptible C57BL/6J (B6J) mice encoding nucleotide substitutions in the *Ob* gene that resulted in the Oβ proteins with single (S128N, V148I and L167H) or double (S128N/V148I and E239K/S240L; B6J mice have unique substitution S240L not found in mice from other backgrounds, Figure 1A) AA changes. Two to three independent founders per each line were bred to B6J mice for two generations. Heterozygous mice from each line were intercrossed to establish homozygous KI lines.

We first confirmed that KI mutations did not result in large alterations in H2-O and H2-M protein levels. Western blotting of B cell lysates from all the KI mice showed only small variations in H2-O and H2-M protein levels compared to the levels in B6J B cells. However, these variations did not change ratios of H2-M:H2-O (Figure 1B; bottom panels and Supplemental Figure 1A). Our previous studies showed that the mutations found in I/LnJ *Ob* did not alter H2-M/H2-O interactions (5). However, it was important to confirm that B6J.*Ob*KI mice produced Oβ that did not impact H2-M/H2-O interactions in isolation from the other I/LnJ genes. Therefore, H2-M and any co-associated H2-O was captured from B6J and B6J.*Ob*KI B cell lysates by immunoprecipitation with a heterodimer-specific anti-H2-M monoclonal Ab followed by western blotting with Abs specific for the Cts of Oβ and Mβ (Figure 1B; left, top panel). In the case of the E239K/S240L double mutant, a polyclonal serum specific for the Oβ luminal domain was used since the KI mutations in the Ct impaired the binding of the Ab specific for the Oβ cytoplasmic tail (Figure 1B; right, top panel). We also performed the converse experiment in which H2-O was immunoprecipitated followed by western blotting for Oβ and Mβ (Figure 1B; middle panels). These experiments revealed similar levels of H2-M co-associated with H2-O as well as similar ratios of H2-M:H2-O in B cells from all B6J.*Ob*KI mice compared to B6J mice (Figure 1B and Supplemental Figure 1B). Thus, these single or double KI AA mutations within Oβ did not alter H2-O or H2-M protein levels or perturb H2-O/H-2M interactions.

Cells that lack H2-O or express I/LnJ H2-O have lower than normal levels of MHCII-CLIP complexes as H2-M function is enhanced in the absence of inhibition by H2-O (5, 27).

Thus, cell surface MHCII-CLIP levels can be used as a read-out to measure the impact of the Oβ AA substitutions on H2-O protein function. Therefore, we used the 15G4 mAb that specifically recognizes I-A^b-CLIP complexes [(15) and Supplemental Figure 1C] to measure MHCII-CLIP levels on splenic B cells from B6J.*Ob* KI mice and B6J control mice (see Supplemental Figure 2 for details). B cells from none of the KI lines exhibited the decrease in MHCII-CLIP levels characteristic of $Ob^{-/-}$ cells (Figure 1C) and cells expressing I/LnJ Oβ (5).

As expected, when challenged with MMTV, none of the B6J.*Ob* KI mice produced virus-neutralizing Ab titers that were comparable to the titers in infected $Ob^{-/-}$ mice (Figure 1D). The V 148I *Ob* allele appears to be a gain of function allele (Figure 1C). However, this was not the mutation driving the virus-neutralizing Ab responses (Figure 1D). Collectively these data show these individual or double mutations in Oβ were insufficient to confer loss of function H2-O.

Identification of three AAs in the Oβ Ig domain as mediating H2-O loss-of-function.

Using a publicly available data base with sequenced genomes of various inbred mouse lines (Sanger Institute Mouse Genomes Project), we found that the *Ob* allele of the wild-derived CAST/EiJ (CAST) mice had the three Ig domain mutations found in I/LnJ mice: S128N, V148I and L167H (Figure 1A). To test whether CAST mice produced virus-neutralizing Abs similar to I/LnJ mice, we injected them with MMTV and screened their sera for the ability to neutralize the virus. Similar to I/LnJ mice, CAST mice produced anti-MMTV Abs (Figure 2A, top) that efficiently neutralized virus (Figure 2A, bottom). These data suggest that the combination of the three mutations found in the CAST *Ob* allele could be sufficient to mediate H2-O loss-of-function. To directly test this possibility, we compared the ability of CAST H2-O to inhibit H2-M function in B cells from (B6J.$Ob^{-/-}$ × CAST)F1 (F1.$Ob^{CAST/-}$) and (B6J × CAST)F1 (F1.$Ob^{CAST/B6}$) (Figure 2B, top) by measuring MHCII-CLIP levels. Importantly, all other genes in F1.$Ob^{CAST/-}$ and F1.$Ob^{CAST/B6}$ mice are heterozygous (one B6 allele and one CAST allele) and thus, could not be considered as contributing to the phenotype. B cells from F1.$Ob^{CAST/-}$ expressed significantly lower levels of MHCII-CLIP compared to F1.$Ob^{CAST/B6}$ B cells (Figure 2B, bottom). These data indicate that the CAST *Ob* allele is a loss-of-function allele. I/LnJ mice have similar levels of H2-O and H2-M protein and H2-M/H2-O interactions appeared to be similar to those in B6J mice, despite I/LnJ *Ob* being a loss-of-function allele (5). Therefore, we next asked if CAST H2-O and H2-M protein levels were normal and H2-O/H2-M interactions were similar to those observed in virus-susceptible BALB/cJ mice (Figure 2C). BALB/cJ mice were used for these studies since the Cts of BALB/cJ and CAST mice are identical, allowing for the use of a polyclonal serum specific for the Oβ Ct tail. CAST mice had, on average, 17% less H2-O than BALB/cJ mice. As a result, the total ratio of H2-M:H2-O was slightly higher as less H2-O co-precipitated with H2-M when H2-M was captured from CAST B cell lysates (Figure 2C and 2D). It is unlikely, however, that this small decrease in H2-O resulted in altered MHCII-CLIP levels because H2-$O^{+/+}$ and H2-$O^{+/-}$ mice (which have a 2-fold difference in H2-O) have similar levels of MHCII-CLIP (28). Nevertheless, to provide more conclusive evidence that CAST mice possess a null allele of *Ob* and, importantly to directly link this the CAST *Ob* allele with the production of virus-neutralizing Abs, we

undertook a genetic approach. Our published studies have demonstrated that two genes in I/LnJ mice are necessary and sufficient to allow for antibody responses to MMTV following neonatal infection (28). The first gene, *vic1*, which encodes the loss-of-function *Ob* allele, is sufficient to confer Ab responses to mice infected as adults. An additional locus, which acts as a modifier of *vic1*, termed *vic2*, confers the ability to produce Abs following natural infection of neonates with MMTV via breastmilk. *Vic2* is dominant and modifies the function of recessive *vic1*, meaning that the presence of two alleles of *vic1* and one allele of *vic2* of the I/LnJ origin are necessary and sufficient to produce Ab responses against MMTV in mice infected as neonates (28). Therefore, to test whether CAST mice have a loss of function *Ob* similar to I/LnJ mice, we generated (I × CAST)F1 and control (I × B6J)F1 and (B6J$^{vic1i/i}$ × CAST)F1 mice and fostered them by viremic mothers as neonates. Both B6J and CAST mice have a susceptible allele of *vic2* [(28) and data not shown]. Thus, only (I × CAST)F1 mice would produce MMTV-neutralizing Abs if I/LnJ and CAST mice have loss-of-function alleles of *Ob*. As expected, only (IxCAST)F1 mice produced virus-neutralizing Abs (Figure 2E, top and bottom), whereas the control F1 hybrids failed to do so. Collectively, these studies identified the three polymorphic AAs in the Ig domain of CAST and I/LnJ Oβ proteins as responsible for the loss of H2-O function.

Novel modifiers of the MHCII pathway.

Our published data (5) and the data presented here suggest that H2-O requires an unknown factor(s) to inhibit H2-M since I/LnJ and CAST H2-O efficiently bind H2-M but yet fail to inhibit H2-M function. If so, then animals with the WT allele of H2-O but without the functional allele of this provisional factor(s) should exhibit the phenotype of H2-O-deficient mice. The inbred mouse strain B6J was established at The Jackson Laboratory in 1948. In 1951, at the F32 generation of inbreeding, it was passed on to the National Institutes of Health, leading to development of the C57BL/6N (B6N) mouse strain. The C57BL/6NTac (B6NTac) sub-strain was established at F151, following the transfer of the B6N line to Taconic Farms in 1991. Unexpectedly, we found that when compared to B6J, both B6N and B6NTac mice have significantly lower MHCII-CLIP levels on the surface of their B cells and DCs, similar to the levels in B6J.*Ob*$^{-/-}$ cells (Figures 3A and 3B, respectively).

Low MHCII-CLIP (MHCII-CLIP^{Low}) levels in B6J.*Ob*$^{-/-}$ mice correlate with production of virus-neutralizing Abs [(5) and Figures 1C and D]. To determine whether the MHCII-CLIP^{Low} levels in B6N mice also correlated with an efficient anti-viral Ab response, we infected B6N and B6J mice with MMTV and three months later screened their sera for virus-neutralizing Abs. B6N (but not B6J) mice produced high titers of anti-MMTV Abs (Figure 3C) that efficiently neutralized the virus (Figure 3D).

To determine whether the mechanism underlying the MHCII-CLIP^{High} phenotype in B6J mice was dominant, we crossed B6J by B6N mice to produce F1 mice. B cells from these F1 mice had MHCII-CLIP levels similar to that of B6J mice (Figure 3A), indicating that the MHC-CLIP^{High} level is a dominant trait. To determine the number of genes controlling the MHCII-CLIP^{High} phenotype in B6J mice, we backcrossed F1 mice to B6N mice to generate N2 mice and measured MHCII-CLIP levels on their splenic B cells. Whereas 89/121 (74%) of N2 mice had levels of MHCII-CLIP comparable to the levels in B6N mice, 32/121 (26%)

had levels similar that of B6J mice (Figure 3A). This distribution of phenotypes indicates that two dominant genes control the MHCII-CLIP^{High} phenotype in B6J mice as only ~25% of N2 mice are expected to have MHCII-CLIP^{High} level and the rest (~75%) are expected to be MHCII-CLIP^{Low} (Figure 3E). In contrast, B6N mice inherit 2 recessive alleles of these genes which we provisionally called class II presentation modifier A and B (*c2pmA and c2pmB*). Our data suggest that H2-O exerts its negative function on H2-M only in mice inheriting dominant alleles of both *c2pmA* and *c2pmB*.

The genomes of B6J and B6N mice have been sequenced (29). Between the two genomes, 51 coding variants that include coding SNPs, insertions and deletions were identified (30) but no polymorphisms were found within the coding regions of H2-M, MHCII, H2-O, invariant chain, or cathepsins S and L (29) indicating that *c2pmA and c2pmB* are not these genes. Moreover, overall levels of H2-O, H2-M, and MHCII in B cells and DCs from B6J, B6N, and B6NTac mice were similar as were H2-O/H2-M interactions (Figure 4A, Figure 4B and Supplemental Figure 3). Thus, B6N and B6J mice inherit identical alleles of known genes that mediate the main functions within the MHCII presentation pathway and yet B6N mice exhibit the MHCII-CLIP^{Low} phenotype characteristic of H2-O-deficient B6J mice.

To test whether *c2pmA* and *c2pmB* are expressed in cells of bone marrow (BM) origin we used a BM chimera (BMC) approach. Lineage marker negative (lin^{-}) B6J BM cells were transferred intravenously (i.v.) into lethally irradiated B6N mice (B6J→B6N). The converse chimeras were also established (B6N→B6J) as well as the requisite control chimeras (B6J→B6J and B6N→B6N). The chimeric mice were sacrificed nine weeks post-transplant and MHCII-CLIP levels on splenic B cells were measured by flow cytometry. The results showed that MHCII-CLIP^{High} levels on B6J B cells remained high on the cells that developed in B6N mice and MHCII-CLIP^{Low} remained low on B6N B cells that developed in B6J mice (Figure 4C). Thus, *c2pmA* and *c2pmB* are expressed in cells of the BM origin.

To determine whether *c2pmA* and *c2pmB* function in B cells, an additional set of BMCs were established in which lethally irradiated B6N mice were reconstituted either with a 50:50 mix of lin^{-} BM cells derived from B6J.μMT (B-less mice) and B6N (the source of B cells) mice or with control B6N BM. At 12 weeks post-transplant, the levels of MHCII-CLIP and MHCII on peripheral blood B cells were measured by flow cytometry (Figure 4D and Supplemental Figure 4). B6N-derived B cells in both groups of BMCs maintained the donor-derived MHCII CLIP^{Low} phenotype. Two possibilities could explain these results. First, *c2pmA* and *c2pmB* could be B-cell intrinsic intracellular factors. Alternatively, *c2pmA* and *c2pmB* could be autocrine factors secreted by B cells and acting upon B cells. However, in either case *c2pmA* and *c2pmB* function in B cells.

Discussion

Since its discovery over two decades ago, considerable work has been done to describe the function and structure of H2-O/DO. Multiple groups have reported H2-O as an inhibitor H2-M and therefore a negative regulator of peptide loading on MHCII-CLIP using *in vitro* cell line and biochemistry-based approaches (10, 31, 32). It has also been demonstrated *in vivo* in mice that successful inhibition of H2-M by H2-O results in a higher proportion

of CLIP-bound MHCII complexes on APCs (5). The inhibitory nature and similarity of H2-O to MHCII in structure suggests H2-O acts as a competitive inhibitor of MHCII:H2-M binding (8). However, previous work from our laboratories demonstrated that H2-O found in mice of the I/LnJ strain was nonfunctional yet maintained interaction with H2-M (5). This indicates that, contrary to the current paradigm, H2-O/H2-M binding alone is not sufficient to block H2-M function *in vivo*.

H2-O is a constitutive heterodimer, composed of Oβ and Oα chain. Compared to the *Ob* allele of retrovirus-susceptible mice, the *Ob* allele of retrovirus-resistant I/LnJ mice encodes for three distinct AA mutations in Ig domain and a single AA mutation in the Ct domain (Figure 1A). We present data demonstrating that *Ob* alleles that encode for single or double AA mutations found in the Ig domain or Ct domain of I/LnJ Oβ do not alter the function of H2-O (Figure 1B and 1C). In contrast, the CAST *Ob* allele that encodes for three Ig AA mutations found in I/LnJ Oβ results in H2-O with loss-of-function (Figure 2A and 2B). Although CAST mice have slightly lower H2-O levels, CAST H2-O retains the ability to interact with H2-M. The fact that this loss-of-function H2-O is still capable of binding to H2-M (Figure 2C) is not surprising as the DM/DO crystal structures shows that DM/DO interactions are mainly driven by contacts between DOα and DM and that the 3 Ig domain mutations likely point away from the DM/DO interface (8). Based on these data we propose that H2-O requires yet to be identified factors to inhibit H2-M and that these factors may interact with the Ig domain of Oβ.

Serendipitously, we also discovered that two closely related strains of B6 mice, B6J and B6N, exhibit different MHCII-CLIP levels in B and DC cells: high in B6J and low in B6N mice (Figures 3A and 3B). The low MHCII-CLIP levels, indicative of uninhibited H2-M in B6N cells, correlated with the production of a potent neutralizing Ab response against a retrovirus (Figure 3C and 3D) as seen in B6J.$Ob^{-/-}$ mice [Figure 1D and (5)]. Genetic crosses between the B6J and B6N mice identified two dominant loci (which we provisionally call *c2pmA* and *c2pmB*) that are inherited by B6J mice and control the MHCII-CLIP^{High} phenotype (Figure 3A and 3E). BMC experiments showed that *c2pmA* and *c2pmB* are expressed in the BM cells and function in B cells (Figures 4C and 4D). Whether these genes function in other cells expressing H2-O remains to be investigated.

c2pmA and *c2pmB* do not encode for H2-M, MHCII, H2-O, invariant chain, or cathepsins L and S as there are no polymorphisms identified between the B6N and B6J alleles of these genes. In addition, as the levels of MHCII, H2-M and H2-O proteins are similar in B6J and B6N B cells as are H2-M/H2-O interactions (Figures 4A, 4B and Supplemental Figure 3), it is unlikely that *c2pmA* and *c2pmB* affect the expression of these MHCII pathway proteins. *c2pm*A and *c2pmB* might potentially encode for genes participating in processes such as trafficking, uptake, and antigen processing or represent negative regulators, enhancers, microRNAs and other control elements. But until these genes are identified it is too premature to discuss their functions.

To our knowledge, this is the first report showing that there are additional factors other than H2-M and H2-O that control peptide loading of MHCII molecules. These data highlight that modulation of antigen presentation by H2-M and H2-O is more complex than previously

appreciated. Our data indicate that binding of H2-M by H2-O is not sufficient for H2-M inhibition as previously suggested (5) and that regions of H2-O distinct from the site of H2-M/H2-O interaction are likely critical for H2-O function. The mechanism underlying H2-O function is still unclear, but H2-O may exert its function by binding to and altering the conformation of H2-M in a manner dependent on the AA composition of the Ig domain of Oβ. The unknown factors encoded by the *c2pmA* and *c2pmB* loci can alter MHCII presentation directly by altering the activity of H2-M, indirectly by modifying the activity of H2-O via targeting the Ig domain, or by altering another yet to be defined pathway. The precise nature of these interactions will be revealed via the positional cloning of genes encoded by *c2pmA* and *c2pmB*.

Supplementary Material

Refer to Web version on PubMed Central for supplementary material.

Acknowledgements

We are thankful to members of the Golovkina, Chervonsky and Denzin laboratories for discussions, Louis Osorio and Dr. Derek Sant'Angelo for technical assistance and Dr. S. Erickson for the help with the design to make *Ob* KI mice.

Funding sources:

This work was supported by PHS grant AI117535 to T. G. and L.K.D., by P30 CA014599 to the University of Chicago, by the National Center for Advancing Translational Sciences of the National Institutes of Health through Grant Number UL1 TR000430 to the University of Chicago.

References

1. Purdy A, Case L, Duvall M, Overstrom-Coleman M, Monnier N, Chervonsky A, and Golovkina T. 2003. Unique resistance of I/LnJ mice to a retrovirus is due to sustained interferon gamma-dependent production of virus-neutralizing antibodies. J Exp Med 197: 233–243. [PubMed: 12538662]
2. Case LK, Petell L, Yurkovetskiy L, Purdy A, Savage KJ, and Golovkina TV. 2008. Replication of beta- and gammaretroviruses is restricted in I/LnJ mice via the same genetic mechanism. Journal of virology 82: 1438–1447. [PubMed: 18057254]
3. Kane M, Case LK, and Golovkina TV. 2011. Vital role for CD8+ cells in controlling retroviral infections. Journal of virology 85: 3415–3423. [PubMed: 21248041]
4. Case LK, Purdy A, and Golovkina TV. 2005. Molecular and cellular basis of the retrovirus resistance in I/LnJ mice. J Immunol 175: 7543–7549. [PubMed: 16301663]
5. Denzin LK, Khan AA, Virdis F, Wilks J, Kane M, Beilinson HA, Dikiy S, Case LK, Roopenian D, Witkowski M, Chervonsky AV, and Golovkina TV. 2017. Neutralizing Antibody Responses to Viral Infections Are Linked to the Non-classical MHC Class II Gene H2-Ob. Immunity 47: 310–322 e317. [PubMed: 28813660]
6. Fung-Leung WP, Surh CD, Liljedahl M, Pang J, Leturcq D, Peterson PA, Webb SR, and Karlsson L. 1996. Antigen presentation and T cell development in H2-M-deficient mice. Science 271: 1278–1281. [PubMed: 8638109]
7. Mellins ED, and Stern LJ. 2014. HLA-DM and HLA-DO, key regulators of MHC-II processing and presentation. Current opinion in immunology 26: 115–122. [PubMed: 24463216]
8. Guce AI, Mortimer SE, Yoon T, Painter CA, Jiang W, Mellins ED, and Stern LJ. 2013. HLA-DO acts as a substrate mimic to inhibit HLA-DM by a competitive mechanism. Nature structural & molecular biology 20: 90–98.

9. Kropshofer H, Vogt AB, Thery C, Armandola EA, Li BC, Moldenhauer G, Amigorena S, and Hammerling GJ. 1998. A role for HLA-DO as a co-chaperone of HLA-DM in peptide loading of MHC class II molecules. The EMBO journal 17: 2971–2981. [PubMed: 9606180]
10. Denzin LK, Sant'Angelo DB, Hammond C, Surman MJ, and Cresswell P. 1997. Negative regulation by HLA-DO of MHC class II-restricted antigen processing. Science 278: 106–109. [PubMed: 9311912]
11. Yoon T, Macmillan H, Mortimer SE, Jiang W, Rinderknecht CH, Stern LJ, and Mellins ED. 2012. Mapping the HLA-DO/HLA-DM complex by FRET and mutagenesis. Proceedings of the National Academy of Sciences of the United States of America 109: 11276–11281. [PubMed: 22733780]
12. van Ham SM, Tjin EP, Lillemeier BF, Gruneberg U, van Meijgaarden KE, Pastoors L, Verwoerd D, Tulp A, Canas B, Rahman D, Ottenhoff TH, Pappin DJ, Trowsdale J, and Neefjes J. 1997. HLA-DO is a negative modulator of HLA-DM-mediated MHC class II peptide loading. Curr Biol 7: 950–957. [PubMed: 9382849]
13. Kremer AN, van der Meijden ED, Honders MW, Goeman JJ, Wiertz EJ, Falkenburg JH, and Griffioen M. 2012. Endogenous HLA class II epitopes that are immunogenic in vivo show distinct behavior toward HLA-DM and its natural inhibitor HLA-DO. Blood 120: 3246–3255. [PubMed: 22889757]
14. Nanaware PP, Jurewicz MM, Leszyk JD, Shaffer SA, and Stern LJ. 2019. HLA-DO Modulates the Diversity of the MHC-II Self-peptidome. Mol Cell Proteomics 18: 490–503. [PubMed: 30573663]
15. Liljedahl M, Winqvist O, Surh CD, Wong P, Ngo K, Teyton L, Peterson PA, Brunmark A, Rudensky AY, Fung-Leung WP, and Karlsson L. 1998. Altered antigen presentation in mice lacking H2-O. Immunity 8: 233–243. [PubMed: 9492004]
16. Welsh RA, Song N, Foss CA, Boronina T, Cole RN, and Sadegh-Nasseri S. 2020. Lack of the MHC class II chaperone H2-O causes susceptibility to autoimmune diseases. PLoS Biol 18: e3000590. [PubMed: 32069316]
17. Graves AM, Virdis F, Morrison E, Alvaro-Benito M, Khan AA, Freund C, Golovkina TV, and Denzin LK. 2020. Human Hepatitis B Viral Infection Outcomes Are Linked to Naturally Occurring Variants of HLA-DOA That Have Altered Function. J Immunol.
18. Miyazaki T, Wolf P, Tourne S, Waltzinger C, Dierich A, Barois N, Ploegh H, Benoist C, and Mathis D. 1996. Mice lacking H2-M complexes, enigmatic elements of the MHC class II peptide-loading pathway. Cell 84: 531–541. [PubMed: 8598040]
19. Piazzon I, Goldman A, Torello S, Nepomnaschy I, Deroche A, and Dran G. 1994. Transmission of an Mls-1a-like superantigen to BALB/c mice by foster-nursing on F1 Mls-1bxa mothers. Sex-influenced onset of clonal deletion. J. Immunol 153: 1553–1562. [PubMed: 7913941]
20. Golovkina TV, Piazzon I, Nepomnaschy I, Buggiano V, de Olano Vela M, and Ross SR. 1997. Generation of a tumorigenic milk-borne mouse mammary tumor virus by recombination between endogenous and exogenous viruses. J. Virol 71: 3895–3903. [PubMed: 9094666]
21. Buggiano V, Goldman A, Nepomnaschy I, Bekinschtein P, Berguer P, Lombardi G, Deroche A, Francisco MV, and Piazzon I. 1999. Characterization of two infectious mouse mammary tumour viruses: superantigenicity and tumorigenicity. Scand. J. Immunol 49: 269–277. [PubMed: 10102644]
22. Marrack P, Kushnir E, and Kappler J. 1991. A maternally inherited superantigen encoded by mammary tumor virus. Nature 349: 524–526. [PubMed: 1846947]
23. Chirgwin JM, Prxybyla AE, MacDonald RJ, and Rutter WJ. 1979. Isolation of biologically active ribonucleic acid from sources enriched in ribonuclease. Biochemistry 18: 5294–5299. [PubMed: 518835]
24. Fallas JL, Yi W, Draghi NA, O'Rourke HM, and Denzin LK. 2007. Expression patterns of H2-O in mouse B cells and dendritic cells correlate with cell function. J Immunol 178: 1488–1497. [PubMed: 17237397]
25. Golovkina T, Agafonova Y, Kazansky D, and Chervonsky A. 2001. Diverse repertoire of the MHC class II-peptide complexes is required for presentation of viral superantigens. J Immunol 166: 2244–2250. [PubMed: 11160278]
26. Finke D, Luther SA, and Acha-Orbea H. 2003. The role of neutralizing antibodies for mouse mammary tumor virus transmission and mammary cancer development. Proceedings of the

National Academy of Sciences of the United States of America 100: 199–204. [PubMed: 12502785]

27. Gu Y, Jensen PE, and Chen X. 2013. Immunodeficiency and autoimmunity in H2-O-deficient mice. J Immunol 190: 126–137. [PubMed: 23209323]
28. Cullum E, Dikiy S, Beilinson HA, Kane M, Veinbachs A, Beilinson VM, Denzin LK, Chervonsky A, and Golovkina T. 2020. Genetic Control of Neonatal Immune Tolerance to an Exogenous Retrovirus. Journal of virology 94.
29. Keane TM, Goodstadt L, Danecek P, White MA, Wong K, Yalcin B, Heger A, Agam A, Slater G, Goodson M, Furlotte NA, Eskin E, Nellaker C, Whitley H, Cleak J, Janowitz D, Hernandez-Pliego P, Edwards A, Belgard TG, Oliver PL, McIntyre RE, Bhomra A, Nicod J, Gan X, Yuan W, van der Weyden L, Steward CA, Bala S, Stalker J, Mott R, Durbin R, Jackson IJ, Czechanski A, Guerra-Assuncao JA, Donahue LR, Reinholdt LG, Payseur BA, Ponting CP, Birney E, Flint J, and Adams DJ. 2011. Mouse genomic variation and its effect on phenotypes and gene regulation. Nature 477: 289–294. [PubMed: 21921910]
30. Simon MM, Greenaway S, White JK, Fuchs H, Gailus-Durner V, Wells S, Sorg T, Wong K, Bedu E, Cartwright EJ, Dacquin R, Djebali S, Estabel J, Graw J, Ingham NJ, Jackson IJ, Lengeling A, Mandillo S, Marvel J, Meziane H, Preitner F, Puk O, Roux M, Adams DJ, Atkins S, Ayadi A, Becker L, Blake A, Brooker D, Cater H, Champy MF, Combe R, Danecek P, di Fenza A, Gates H, Gerdin AK, Golini E, Hancock JM, Hans W, Holter SM, Hough T, Jurdic P, Keane TM, Morgan H, Muller W, Neff F, Nicholson G, Pasche B, Roberson LA, Rozman J, Sanderson M, Santos L, Selloum M, Shannon C, Southwell A, Tocchini-Valentini GP, Vancollie VE, Westerberg H, Wurst W, Zi M, Yalcin B, Ramirez-Solis R, Steel KP, Mallon AM, de Angelis MH, Herault Y, and Brown SD. 2013. A comparative phenotypic and genomic analysis of C57BL/6J and C57BL/6N mouse strains. Genome biology 14: R82. [PubMed: 23902802]
31. Denzin LK, and Cresswell P. 1995. HLA-DM induces CLIP dissociation from MHC class II alpha beta dimers and facilitates peptide loading. Cell 82: 155–165. [PubMed: 7606781]
32. Liljedahl M, Kuwana T, Fung-Leung WP, Jackson MR, Peterson PA, and Karlsson L. 1996. HLA-DO is a lysosomal resident which requires association with HLA-DM for efficient intracellular transport. The EMBO journal 15: 4817–4824. [PubMed: 8890155]

Key Points

1. Three key H2-Oβ Ig-domain residues control H2-O function
2. MHCII presentation and anti-viral Ab responses are diverse in B6J and B6N mice
3. Two non-MHC loci mediate the difference in MHCII presentation in B6J and B6N mice

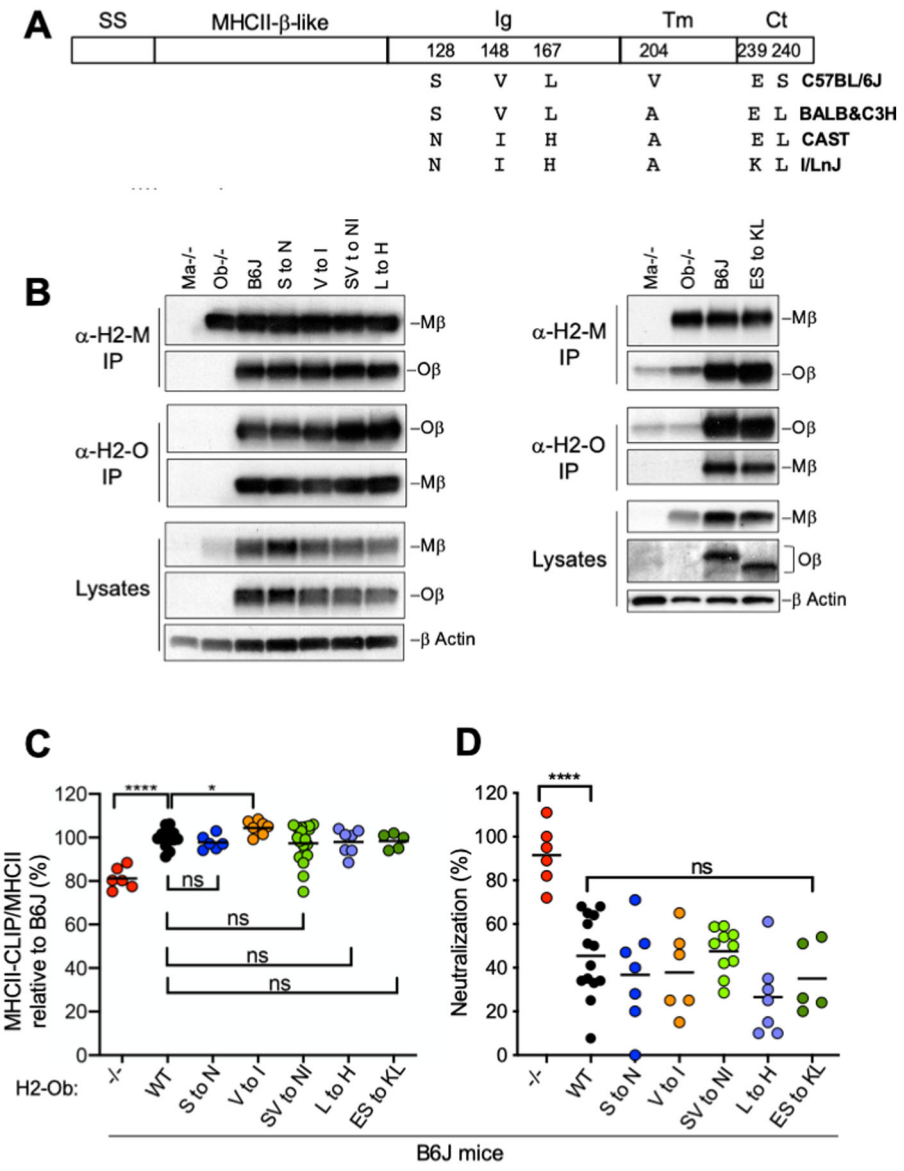

Figure 1. Oβ proteins with single or double mutations in the Ig domain or cytoplasmic tail do not affect H2-O function.

(A) The domain structure of Oβ: SS, signal sequence; MHCII β-like, MHCII β like domain; Ig, immunoglobulin domain; Tm, transmembrane domain; Ct, cytoplasmic tail. Also shown: AA substitutions (and their positions) found in Oβ from various mice compared to Oβ of B6 mice. **(B)** Oβ and Mβ protein levels and H2-M/H2-O interactions in *Ob*.KI mice. H2-M or H-2O captured by immunoprecipitation from lysates of purified B6J, B6J.*Ob* S to N, B6J.*Ob* V to I, B6J.*Ob* SV to NI, B6J.*Ob* L to H, and B6J.*Ob* ES to KL splenic B cells were analyzed by western blotting with Abs specific for the Ct of Mβ and Oβ (left panel) or the Ct of Mβ and Oβ luminal domain (right panel) and also for β-actin (loading control). Purified B6J.$Ma^{-/-}$ and B6J.$Ob^{-/-}$ B cells were used as controls. Data are representative of 4 (left panel) and 4 (right panel) independent experiments. See Supplemental Figure 2 for quantification of results across all experiments. **(C)** Comparison of MHCII-CLIP levels

on B cells of *Ob*.KI mice. Quantification of the geometric mean fluorescence intensity (gMFI) of I-A^b-CLIP on B cells, defined as $CD19^+$ from homozygous *Ob* KI mice relative to that obtained for control WT (WT/WT and WT/KI) B6J B cells. To correct for small differences in total MHCII levels among different samples, the ratio of MHCII-CLIP:(total) MHCII was calculated by dividing the gMFI obtained for MHCII-CLIP by that obtained for MHCII for each sample. Graphs show quantification of the gMFI of MHCII-CLIP/MHCII for mice from the indicated strains relative to that obtained for B6J mice. Dots represent individual mice. The data are combined from multiple independent experiments. Horizontal lines indicate the mean of values obtained for each group of mice. **(D)** Mice with indicated genotypes were infected with MMTV at 8 weeks of age (via i.p. injection) and their sera were screened for capacity to neutralize virus at 3 months post-infection. Neutralization (%) was calculated as described in (5). Dots represent individual mice. Horizontal lines indicate the mean of values obtained for different mice from the same group. Significance was calculated using an unpaired *t* test. ****=$p \leq 0.0001$; *=$p \leq 0.05$.

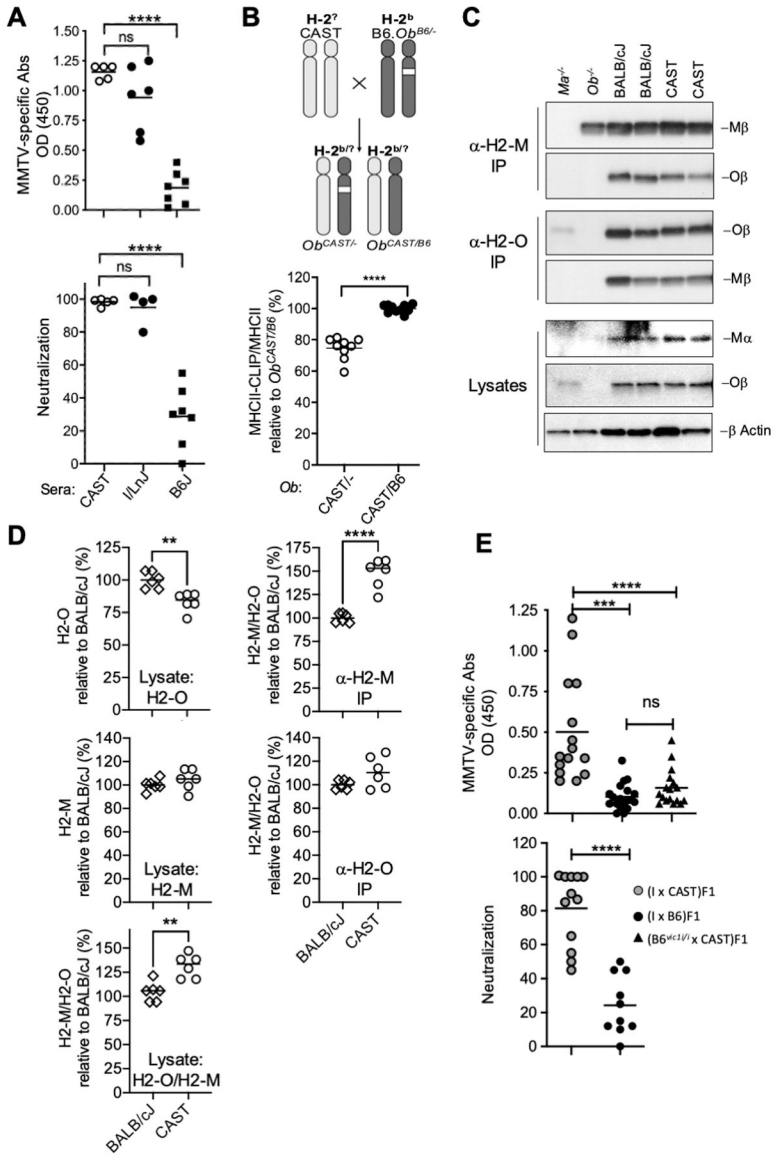

Figure 2. Identification of the combination of mutations within the immunoglobulin domain of Oβ that result in the loss-of-function H2-O.

(A) Similar to I/LnJ mice, MMTV-infected CAST mice produce virus-neutralizing Abs. CAST mice were infected with MMTV at 8 weeks of age (via i.p. injection), and their sera were screened for anti-virus IgGs **(top panel)** and for virus neutralization 3 months post-infection **(bottom panel)**. OD 450, absorbance at 450 nm. Each symbol represents an individual mouse. Horizontal lines indicate the mean of values obtained for mice from the same group. **(B)** Like I/LnJ mice, CAST mice inherit loss-of-function H2-O. **(B, top panel)** Genetic cross to produce H-2$^{?/b}$ $Ob^{CAST/-}$ and H-2$^{?/b}$$Ob^{CAST/B6}$ F1 mice, the CAST MHC haplotype is unknown. **(B, bottom panel)** Quantification of the gMFI of MHCII-CLIP on B cells, identified as CD19^{+} from F1.$Ob^{CAST/-}$ mice relative to that obtained for F1.$Ob^{CAST/B6}$ B cells. To correct for small differences in total MHCII levels among different samples, the ratio of MHCII-CLIP:(total) MHCII was calculated by dividing the gMFI obtained for MHCII-CLIP by that obtained for MHCII for each sample. Graphs show quantification

of the gMFI of MHCII-CLIP/MHCII for mice from both groups relative to that obtained for F1.$Ob^{CAST/B6}$ mice. Each symbol represents an individual mouse. Data are combined from two independent experiments. Horizontal lines indicate the mean of values obtained for each group of mice. **(C)** H2-O and H2-M protein levels and H2-M/H2-O interactions in CAST mice. H2-M or H2-O captured by immunoprecipitation from lysates of purified BALB/cJ and CAST splenic B cells were analyzed by western blotting with Abs specific for the Ct of Mβ and Oβ. Purified B6J.$Ma^{-/-}$ and B6J.$Ob^{-/-}$ B cells were used as controls. Total lysates were also probed by western blotting with Abs specific for Mα, the Ct of Oβ and β-actin (loading control). BALB/cJ and CAST Oβ proteins have identical Cts allowing for the use of Oβ Ab reagents specific for the Ct to perform these analyses. Data are representative of three independent experiments comprised of 2 BALB/cJ and 2 CAST mice each. (**D**) Quantification of total H2-O (top left) and H2-M (middle left) protein levels, the ratio of H2-M to H2-O (bottom left) in B cell lysates and H2-M:H2-O ratios measured after immunoprecipitation with H2-M (top right), or H2-O (bottom right) across the three independent experiments. Data are normalized to the levels obtained for BALB/cJ mice (see Materials and Methods for details). Each symbol represents an individual mouse and horizontal bars represent the mean of values obtained for different mice of the same group. (**E**) Newborn mice from the indicated crosses were fostered by MMTV(LA)-infected mothers. Four months post infection, mice were confirmed to be infected by measuring deletion of SAg-cognate T cells and were screened for anti-virus Abs by ELISA (top panel) and neutralization of MMTV (bottom panel). OD 450, absorbance at 450 nm. Neutralization (%) was calculated as described in (5). Results are expressed as mean of OD (top panel) or as mean of percent of neutralization (bottom panel) produced by sera from uninfected mice of the same cross. Significance was calculated using unpaired *t* tests. ****=p ≤0.0001, ***=P ≤ 0.001, **=P ≤ 0.01.

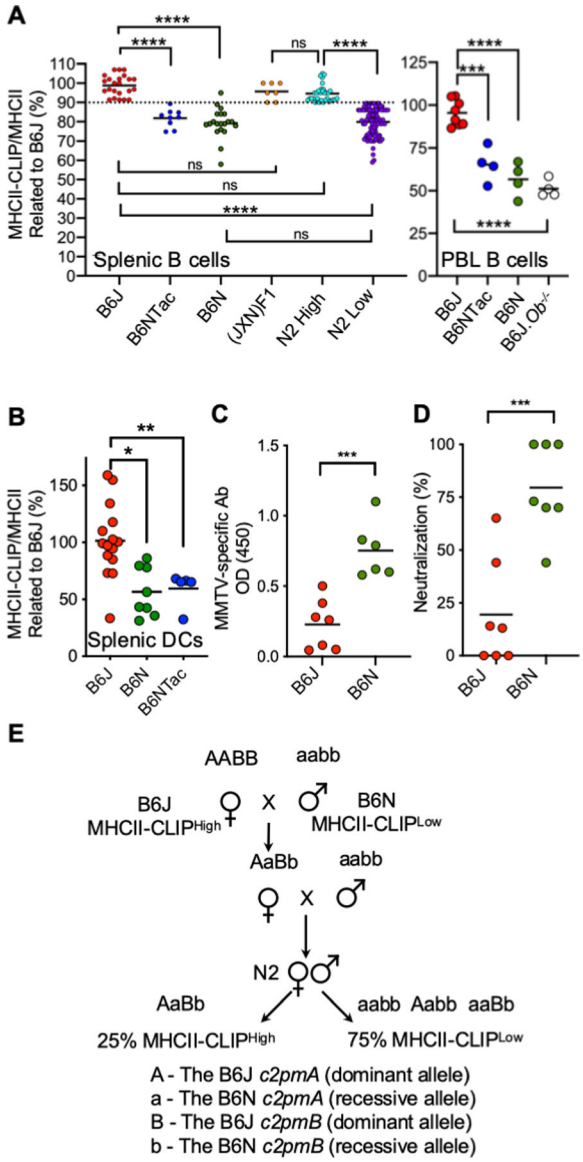

Figure 3. Low MHCII-CLIP levels on B cells and dendritic cells of B6N mice correlates with their ability to produce virus-neutralizing antibodies.

(A) Comparison of MHCII-CLIP levels on splenic B cells of B6N, B6J, F1, and N2 mice **(left)** and on B cells among peripheral blood lymphocytes (PBLs) **(right)**. F1, mice obtained from crossing B6J to B6N mice. N2, mice obtained from backcrossing F1 mice to B6N mice. N2 mice were analyzed in groups (~10–20 mice per group) at 8 weeks of age along with age-matched B6J mice (3–5 mice per group) and their splenic B cells, identified as $CD19^{+}$ were stained with 15G4 (MHCII-CLIP) or M5/114 (total MHCII). To correct for small differences in total MHCII levels among different samples, the ratio of MHCII-CLIP:(total) MHCII was calculated by diving the gMFI obtained for MHCII-CLIP by that obtained for MHCII for each sample. The averaged MHCII-CLIP/MHCII gMFI obtained for B6J mice was defined as 100%. Data for all mice are expressed as % of B6J gMFI. The values for B6J mice ranged from 91.4% to 107% (mean ± SD= 98.8 ± 5.3). The values for B6N ranged from 58% – 95% (mean ± SD= 79.3 ± 7.8). The values for (B6JxB6N)F1

mice ranged from 90%–110% (mean ± SD= 95.6 ± 4.5). With an arbitrary cut off at 90% (dotted line) all N2 MHCII-CLIP^{HIGH} were at ≥ 90% and all N2 MHCII-CLIP^{Low} are at ≤89.5% relative to B6J mice. The range of N2 MHCII-CLIP^{High} was 90% – 105% (mean ± SD= 94.6 ± 4.4), whereas the range of N2 MHCII-CLIP^{Low} was 59% – 89.5% (mean ± SD= 79.9±7.2). Dots represent individual mice. Horizontal lines indicate the mean of values obtained for different mice from the same group.

(B) Quantification of the gMFI of A^{b}-CLIP on the cell surface of splenic DCs from mice of indicated strains and crosses. To correct for small differences in total MHCII levels among different samples, the ratio of MHCII-CLIP:(total) MHCII was calculated by dividing the gMFI obtained for MHCII-CLIP by that obtained for MHCII for each sample. Graphs show quantification of the gMFI of MHCII-CLIP/MHCII for mice from indicated strains/crosses relative to that obtained for B6J mice. B cells were defined as CD19^{+} and DCs as CD3^{-} CD19^{-} CD11c^{+}. Dots represent individual mice. Horizontal lines indicate the mean of values obtained for each group of mice. **(C)** Unlike B6J mice, MMTV-infected B6N mice produce potent virus-neutralizing Abs. B6N and B6J mice were infected with MMTV at 8 weeks of age and screened for anti-virus IgGs 3 months later. OD 450, absorbance at 450 nm. Dots represent individual mice. Horizontal lines indicate the mean of values obtained for different mice from the same group **(D)** Sera from mice (shown in C) were tested for virus neutralization. Dots represent individual mice. Horizontal lines indicate the mean of values obtained for different mice form the same group. **(E)** Genetic cross used to produce N2 mice for *c2pmA* and *c2pmB* mapping.

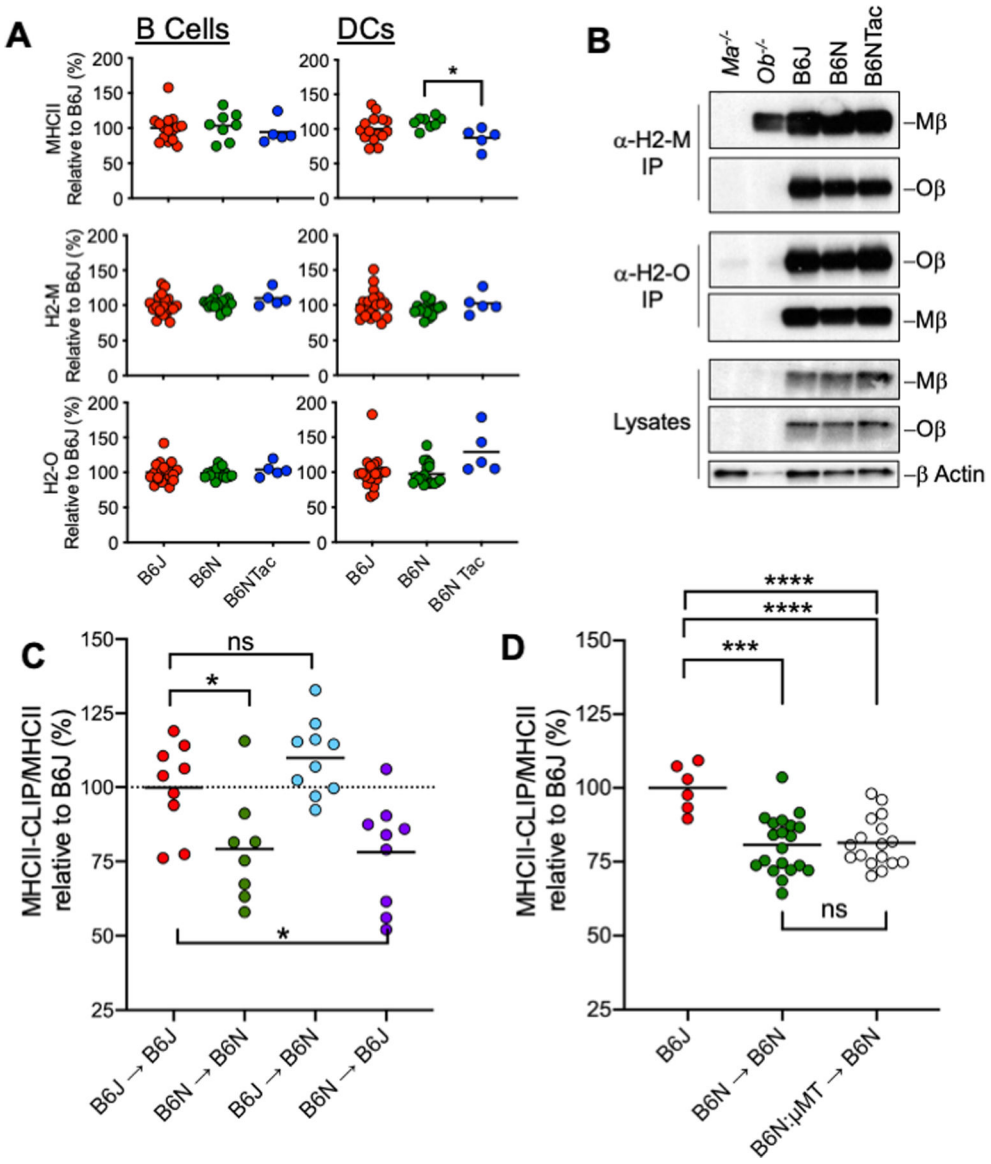

Figure 4. *c2pmA* and *c2pmB* are expressed in the bone marrow compartment and function in B cells.

(A) MHCII, H2-M, and H2-O levels are similar in B6J, B6N, and B6Tac B cells and DCs. Splenic B cells were surface stained with fluorochrome labeled mAbs to identify B cells (CD3- CD11c- CD19+) or DCs (CD3- CD19- CD11c+) and for MHCII followed by fixation and permeabilization and intracellular staining with fluorochrome labeled mAbs specific for H2-O (mAb Mags.Ob3) and H2-M (mAb 2C3A) (see Supplemental Figure 3). Graphs show quantification of the geometric mean fluorescence intensity (gMFI) of MHCII, H2-O, or H2-M in indicated strains of mice relative to that obtained for B6J. Horizontal lines indicate the mean of values obtained for different mice from the same group. Dots represent individual mice. Data were combined from two (MHCII) or 3 (H2-O and H2-M) similar experiments. **(B)** *c2pmA* and *c2pmB* do not alter levels of H2-M, H2-O or MHCII. H2-M or H2-O captured by immunoprecipitation from lysates of purified B6J, B6N and B6NTac, B6J.$Ob^{-/-}$ or B6J$Ma^{-/-}$ splenic B cells were analyzed by blotting with Abs specific for the

cytoplasmic tails of Mβ or Oβ or β-actin. Blotting of lysates used for the IPs are included as controls. Data are representative of 2 similar experiments. See Supplemental Figure 3C for quantification of cumulative data. **(C)** *c2pmA* and *c2pmB* are expressed in cells of the bone marrow origin. Six-week-old B6J or B6N recipient mice were lethally irradiated and reconstituted with lin^- donor B6J or B6N BM. Nine weeks post-transplantation the levels of MHCII and MHCII-CLIP were measured on the surface of $CD19^+$ splenic B cells from the chimeric mice. To correct for small differences in total MHCII levels among different samples, the ratio of MHCII-CLIP:(total) MHCII was calculated by dividing the gMFI obtained for MHCII-CLIP by that obtained for MHCII for each sample. Graphs show quantification of the gMFI of MHCII-CLIP/MHCII for mice from different groups relative to that obtained for B6J mice. Dots represent individual mice. Horizontal lines indicate the mean of values obtained for different mice from the same group. Data were pooled from two independent experiments. **(D)** *c2pmA* and *c2pmB* function in B cells. Six-week-old B6N recipient mice were lethally irradiated and reconstituted with lin^- donor B6N (control) BM or a 50:50 mix of lin^- BM from B6J.μMT (B-less mice) and B6N BM. Twelve weeks post-transplantation the levels of MHCII and MHCII-CLIP were measured on the surface of $CD19^+$ peripheral blood B cells or splenic B cells (Supplemental Figure 4) from the chimeric mice. To normalize each sample's MHCII-CLIP level to this sample's level of MHCII, the gMFI obtained for 15G4 (MHCII-CLIP) was divided by the gMFI obtained for M5/114 (MHCII). Graphs show quantification of the gMFI of MHCII-CLIP/MHCII for mice from different groups relative to that obtained for B6J mice. Data were pooled from two independent transplantation experiments. Dots represent individual mice. Horizontal lines indicate the mean of values obtained for different mice of the same group. Significance was calculated using an unpaired *t* test. ***=$p \leq 0.001$; ****=$p \leq 0.0001$.